7th International Symposium of Marine Propulsors
SMP 2022, Wuxi, China, October 17-21, 2022

Model Scale Investigation of Blade Root Cavitation Erosion on a Set of Marine Propellers

Afaq Ahmed Abbasi [1], Giovanni Franzosi [1], Daniele Bartetta [2], Marina Delucchi [3], Michele Viviani [1]and Giorgio Tani [1]

[1]Department of Electrical, Electronic, Telecommunications Engineering and Naval Architecture, University of Genoa, 16145, Genoa, Italy

[2]Fincantieri S.p.A. Naval Vessel Business Unit, 16000 Genoa, Italy

[3] Department of Civil, Chemical and Environmental Engineering, University of Genoa, 16145, Genoa, Italy

ABSTRACT

The present study is focused on the experimental analysis of the erosion caused by cavitation occurring at the blade root for a set of three model scale marine propellers. The experimental method is based on the adoption of soft paint technique together with cavitation observations. Cavitation dynamics and erosion damage patterns are recorded using three standard cameras and one high speed camera. Standard cameras are fixed on the top of test section to continuously monitor the effect of erosion damage on the blade root, the high-speed camera has been placed at different positions to investigate detailed evolution and collapse of bubbles on pressure and suction side of propeller blades. The soft paint test damage patterns have been simultaneously analysed with the high-speed videos, and results showed remarkable agreement between the occurrence of damage on the blades and the bubble collapse of cavitation. The damage pattern and cavities collapse seem to be inversely related with the inception time of damage.

Keywords

cavitation, marine propellers, cavitation erosion, soft paint test, blade root.

1 INTRODUCTION

For marine propellers, cavitation erosion is one of the most damaging effects of cavitation, which results in efficiency loss, reduction of operating life of propellers and higher overall maintenance cost (Sreedhar, Albert & Pandit 2017). Cavitation erosion is caused by continuous collapse of the cavities near the surface, which impinges high mechanical loads and increased external stresses on the surface (Koukouvinis et al 2017). Hence, designers of marine propellers put all their efforts in designing propellers such to avoid cavitation erosion in their opera-ting conditions.

The occurrence of cavitation erosion is associated with micro-scale mechanism and macro-scale hydrodynamic mechanism related to aggressive bubble collapse. On micro-scale, it has been identified in the literature that bubble collapse will either create a shock wave or microjet structure, depending on the shape of bubble collapsing near the surface (Franc & Michel 2006). Generally spherical shaped bubble collapse results in generation of shock wave (Fujikawa & Akamatsu 1980), and non-spherical shaped bubble collapse results in formation of microjet due to uneven pressure gradient around the collapse (Johnsen & Colonius 2009). The interaction of shock wave and microjet structure results in increased external stresses and jet cutting pressure, respectively. This interaction severely damages the surface, and results in cavitation erosion (Sreedhar, Albert & Pandit 2017). Besides micro-scale mechanism, the research has also focused on macro-scale hydrodynamic phenomena involved in erosive collapse.

High speed visualisation and paint tests have been used synchronously to study the aggressiveness of cavitating flows at macro-level using venturi (Dular & Petkovsek 2015), hydrofoil (Van-Rijsbergen el al 2012), twisted foil (Cao et al 2017) and model propellers (Bensow, Bark & Lu 2012). Based on high speed visualization, Dular & Petkovsek (2015) identified the most erosive cavitating phenomena occurring in a venturi as: cloud cavity collapse, horse-shoe vortex collapse, twister vortex collapse, micro-bubbles collapse on the closure of the sheet cavity, and micro-cavities collapse within break-up region of the cloud cavity. For hydrofoil, cloud cavitation collapse has been identified as an erosion driving

mechanism (Van-Rijsbergen el al 2012). Cao et al (2017) experimentally studied cavitation erosion on a twisted foil and revealed severe paint removal and erosion damages in the vicinity of closure line of sheet cavity, as the flow detaches and collapse in that region.

Model propellers have been experimentally studied using paint tests to create a practical correlation between model scale results and cavitation occurrence at full scale. Blade root cavitation was analysed by Bensow, Bark & Lu (2012), where the cavity collapse and rebounds were thoroughly analysed highlighting the importance of the collapse of large cavities, such as sheet or glassy cavities. Propeller blade root cavitation was analysed also in another study, where cavitation erosion associated to single bubble cavitation at propeller blade root was studied (Abbasi et al 2022). In that work, the collapse of cavities, most of which characterised by twisting motion, in the blade wake was identified as the major contribution to the erosion occurring on the hub immediately downstream of blade root. Based on literature, further studies are needed on propellers to get deep insights of cavitation erosion.

In this paper, the mechanism of cavitation erosion for root bubble cavitation on a series of three propellers is investigated. These test cases are characterised by different cavitation extents and collapse dynamics. This research addresses two main aims: enlarging the knowledge about hydrodynamic mechanisms responsible of cavitation erosion occurring at blade root and assessing a simple experimental procedure able to measure the erosion risk associated to cavitation in order to create a correlation with full scale data.

The availability of this correlation would provide a useful criterion to assess the acceptability of dangerous cavitation phenomena, which is of utmost importance for designing high performance propellers.

2 EXPERIMENTAL OVERVIEW AND SETUP

2.1 UNIGE Cavitation Tunnel and Propellers

The experiments are carried out in cavitation tunnel at UNIGE. It is a Kempf & Remmers closed water circuit cavitation tunnel with test section dimensions of height x width x length = 0.57 m x 0.57 m x 2 m. The nozzle contraction ratio of the tunnel is 4:6:1, which helps in achieving maximum velocity of 8.5 m/s in the tunnel test section. The distance between horizontal and vertical ducts of tunnel are 4.54 m and 8.15 m respectively.

Table 1. Parameters of propellers used in present study

Propeller	Propeller Diameter	Pitch Ratio at 0.7R	Number of Blades	Expanded Blade Area Ratio
P1	0.23	1.3	4	0.7
P2	0.25	1.4	4	0.75
P3	0.25	1.45	4	1.25

The tunnel is equipped with Kempf & Remmers H39 dynamometer, which helps in measuring the thrust, torque, and rate of revolution of propeller. More details about the tunnel can be found here (Tani et al 2017).

Three different four bladed model propeller have been used in the present study. The main parameters of the propellers are given in Table 1.

The propellers have been mounted downstream of dynamometer, with an inclination of 6.5 degrees for P1, 6 ° for P2 and P3. The dynamometer has been positioned in a way to keep the propeller vertically in the centre of the test section. The longitudinal position of the propeller in test section is such that to ensure good optical access from the observation windows of the tunnel. The total run time of propeller for each test in cavitation tunnel was around 200 minutes.

The water quality in the cavitation tunnel is monitored by means of a Metrohm 913PH/DO meter equipped with an O2 Luminophore sensor. A degassing procedure is adopted to control the water quality in the tunnel. The adopted criterion for water quality is to use an oxygen content such to achieve saturation in the high vacuum conditions considered during tests. For current cases this meant oxygen levels varying from 3.8 ppm to about 4.4 ppm.

2.2 Paint Method

A set of guidelines and procedures for painting of propellers for cavitation erosion tests has been recommended by ITTC. As a part of the process, the model is covered by uniform layer of soft paint and is subjected to cavitation in the cavitation tunnel for a certain time. Any damage of the paint connected with the action of collapsing cavities should be considered as a risk of erosion occurrences (ITTC 2011).

In the present study for all the test cases, the propeller has been painted using Diagraph GS ink, as suggested also in (Pfitsch et al 2009), following the complete procedure proposed by ITTC. The propeller model was coated with single layer of paint using a precision spray gun to ensure uniformity, with identical paint coating on all blades. After the application of paint coating, detailed visual inspection was carried out before starting the tests to ensure the quality of paint coating. Based on the visual inspection, it can be stated that before all the tests, the coating was uniform and apparently free of damage that could be confused with damage from erosion or that could trigger anomalous cavitation. After the application of paint, the propeller is left for about seven days for paint to be completely dried.

2.3 Image Acquisition

Three standard cavitation observation cameras (Allied Vision Tech Marlin F145B2) and one high speed camera (Phantom VEO710L equipped with a CMOS sensor) have been used in the present study. Two LED based powerful light (GSVITEC Multiled) have been used to illuminate the field of view of the high high-speed camera, operating them in pulsed mode. Standard cavitation observation cameras are named as CAM0,

CAM1 and CAM2 in this paper, while Fast Cam will be used for referring high speed camera.

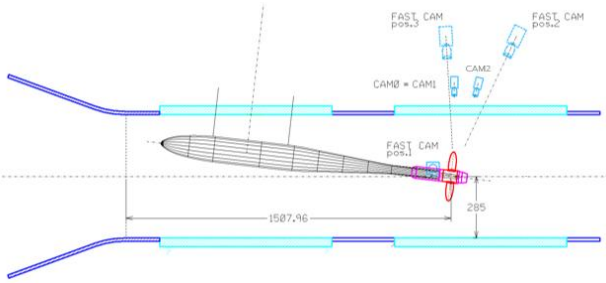

Figure 1. Experimental setup used in present study

CAM0, CAM1 and CAM2 acquired images at resolution of 1392x1040 pixels with maximum sampling frequency of 10 fps. These three cameras have been fixed on the top of the test section focusing the suction side at 90 degrees (CAM 1 and CAM2) and the pressure side at 270 degrees (CAM0). The images acquired with these cameras provide general indications about the damages of the cavitation in order to periodically monitor the paint condition during the experiments.

Fast Cam has maximum resolution of 1280 x 800 pixels and maximum frequency of about 7500 fps at maximum resolution. The fast camera is placed on the side of test section focusing on the suction side blade root for all the tests. During the experiments, two different acquisitions were recorded for each test case, considering these combinations of image size and acquisition frequency (1) 1280 x 800 pixel, frame rate 7500 fps, (2) 448 x 400 pixel, frame rate 34000 fps.

3 CAVITATION OBSERVATION AND VISUALIZATION

The characteristics and behaviour of cavitation occurring at blade root for all the studied test cases are described in this section, providing an overview of the mechanisms likely responsible for erosion and hence of expected damages on the propeller. Propellers considered in the present study exhibit root bubble cavitation ranging from moderate to severe cavitation, and the focus of the study is to observe the effect of root bubble cavitation on the propeller erosion.

Before starting the description of cavitation, it is necessary to provide a brief description of the subject of photographs used in this work. Actually, interpretation of photographs is not straightforward, because the propeller is painted black in colour and not entirely visible in the photographs. The focus of high speed videos was always on the blade root during the passage through the 90 ° position, therefore in the centre of the photographs the hub surface is visible, together with blade root. Pressure side and suction side are both visible, depending on the blade angular position, but focus is on suction side. The outer part of the blades as well as tip vortex cavitation are also visible in most of the photographs, however they are out of focus. Figure 2, perfectly exemplify this characteristic framing. Interpretation of Figure 4 and Figure 6 is slightly more complex because of the closer view to the blade root and of the larger cavitation making the images more confused.

Cavitation observed on P1 propeller has been thoroughly described in (Abbasi et al 2022). This is moderate root bubble cavitation, consisting of one or few separate bubbles occurring at blade root around 90 °, for most of the blade passages. The overall global cavitation on suction side for P1 is shown in Figure 2. Interestingly, bubbles were not observed for all the blade passages, i.e., in some cases there were passages without any root bubble collapse. The cause of this cavitation intermittency can by reasonably attributed to scale effects mostly related to water quality, which are usually more critical for cavitating conditions close to inception.

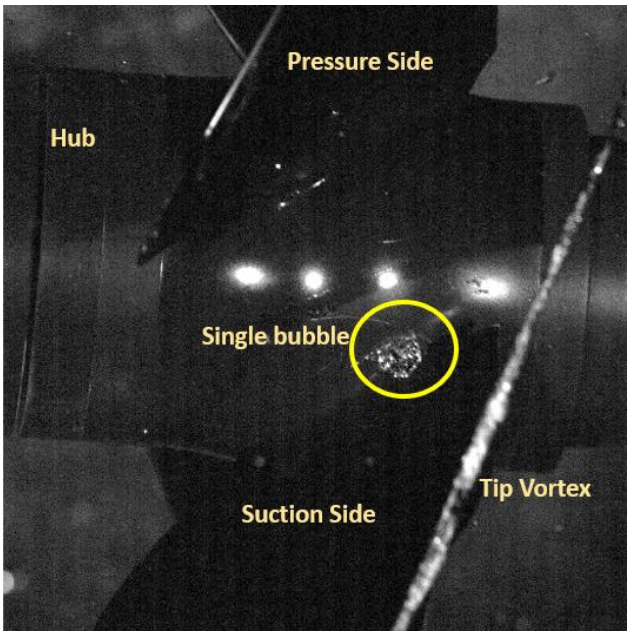

Figure 2. Global cavitation on suction side root for P1 Propeller (flow is from left to right)

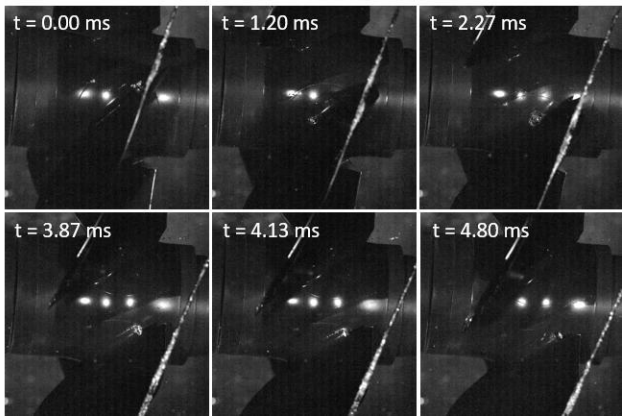

Figure 3. Cavities dynamics (structure, evolution and collapse) for P1 Propeller

The dynamics of cavities for P1 propeller is reported in sequence of frames showing evolution and collapse of a bubble. In most cases bubbles behave as single bubble, generated between the leading edge and mid-chord and

the volume of bubble grows while they are convected downstream. The maximum of the volume is reached around the 75% of the chord, that is at time 2.27 ms in the sequence. Then the volume of the bubble contracts, gradually at first, then suddenly while the bubble reached the trailing edge where collapse occurs.

The collapse occurs in slightly different forms depending on the size and location of the bubble. Larger cavities destabilize from the centre, creating a number of minor cavities, some of them usually collapse with a rapid volume contraction towards the point where paint removal is observed, i.e., a small area at the trailing edge of the blade fillet, including also part of the hub surface.

Smaller bubbles often collapse in the same region, especially those that apparently acquired some twisting motion approaching the trailing edge.

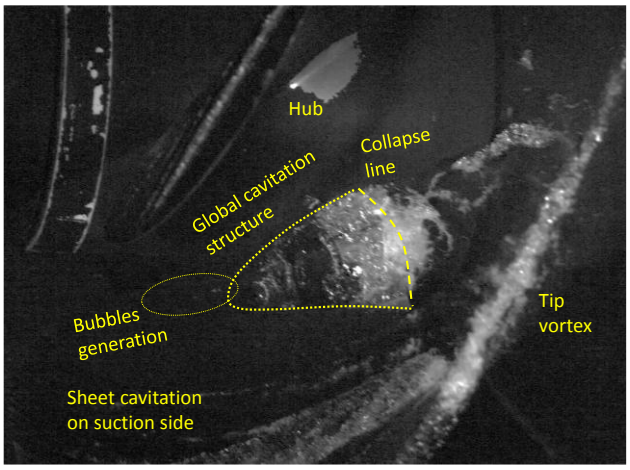

Figure 4. Global cavitation on suction side root for P2 Propeller (flow is from left to right)

For P2 propeller bubble cavitation has been observed on the blade root. Suction side root bubbles are continuously generated between the leading edge and mid-chord. During their motion downstream coalescence occur in between them, and a complex structure extending from the hub surface to about 0.5 R, with a shape similar to that of a wedge. The sub-structures detectable on the irregular surface of this bubble assembly are convected downstream until they reach the cloudy trailing edge of this cavity. Here bubbles are continuously destroyed by collapse taking the appearance of a collapse line. This complex collapse process generates minor cloudy cavities and twisting vortexes, some of which collapse on the hub while the others are convected downstream.

The collapse line here described is easily identified in videos by the apparent motion of the downstream part of bubbles interface against the upstream part: while the upstream part of the bubble is still convected by the flow, the downstream part contracts in the opposite direction generating this cloudy collapse region.

Collapses occur mostly in the space between the overhang and the hub, however many events impinge also on the hub itself and on the blade surface, between the trailing edge and the overhang edge.

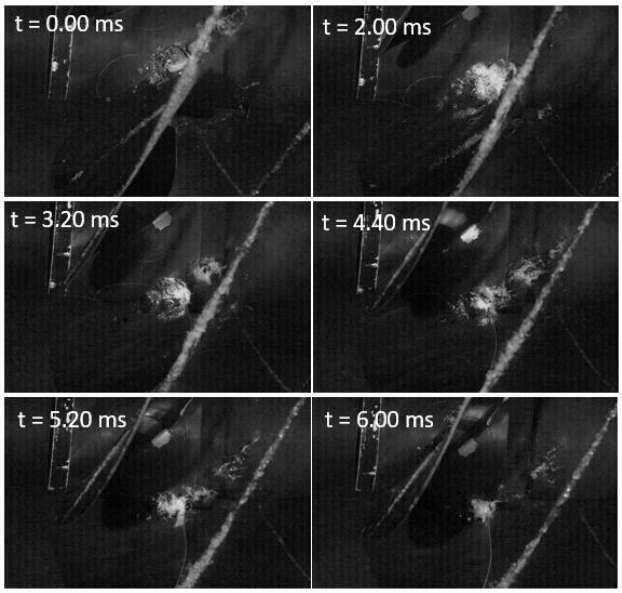

Figure 5. Cavities dynamics (structure, evolution and collapse) for P2 Propeller

Figure 5 reports a sequence of frames describing the evolution of this global cavitation structure for P2 propeller.

In this short sequence, the structure size increases and reaches its maximum at 2 ms, then it starts contracting again towards the blade root (3.2 ms and 4.4 ms). During this contraction of the main cavity, the collapse of minor cavities is observed out of the outer edge of the main cavity, often generating cloudy structure and rebound events (5.2 ms). Vortex structures are shed, which later collapse in the water without creating any damage as they are away from the surface of propeller and hub.

Finally, in the last frame some cavitation is still present close to the root fillet (6 ms). From the visual inspection of the propeller, as well as from the analysis of videos taken by other positions, it is observed that suction side cavitation does not completely collapse. Its size is maximum around 90 °, then it reduces violently moving towards 180 °, but without global collapse of the cavity; the cavitation volume decreases further while passing through 270 °and finally 0 °, when it starts growing again.

Due to this, it can be argued that cavitation erosion for propeller P2 is mostly ascribed to the continuous collapse of the cavitating sub-structures forming the wedge like assembly, rather than to the collapse of the assembly itself.

It is worth mentioning that severe root cavitation was observed for propeller P2 also on the pressure side. This explains the large damage of the paint visible on the pressure side, e.g. in Figure 4. In this work, most of the attention is focused on the analysis of the erosion associated to suction side root cavitation, therefore this phenomenon will not be further analysed.

P3 propeller exhibited heavy cavitation at the blade root. The aspect of suction side root cavitation for this propeller is rather similar to that described for P2: bubbles are continuously generated at leading edge; they grow while moving downstream and they merge forming a wedge like structure whose thickness increases downstream until the collapsing region is reached at blade trailing edge.

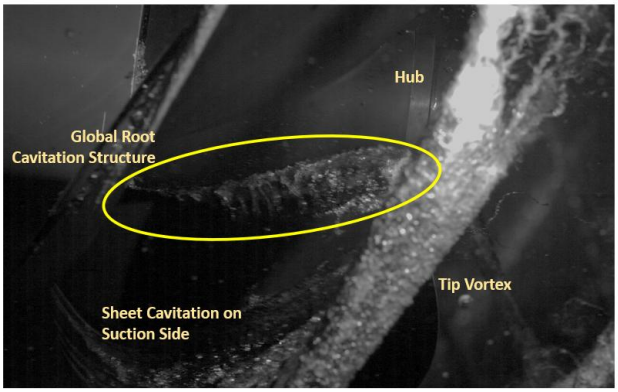

Figure 6. Global cavitation on suction side root for P3 Propeller (flow is from left to right)

Compared to the one observed for propeller P2, root cavitation of propeller P3 is characterised by a higher bubble production rate, with the bubble assembly extending from the leading edge for the whole length of the chord. However, in this case the cavitation evolution during blade rotation is completely different, as it can be seen in Figure 7.

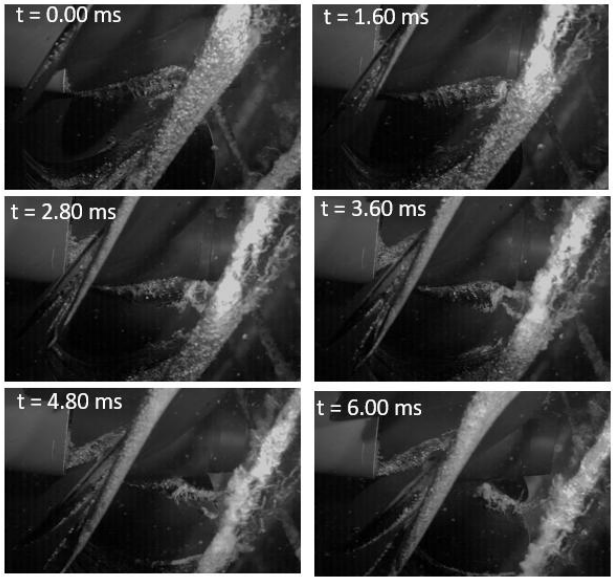

Figure 7. Cavities dynamics (structure, evolution and collapse for P3 Propeller

Actually, after reaching the maximum extent around 90 °, the global cavitation structure contracts violently in all the directions toward a region located approximately at 0.4R, and 0.4C, where violent collapse events are observed. During this process, secondary collapses are observed along the outer edge of the wedge like cavity, associated to the fragmentation of the main cavity during its contraction.

After the collapse of the main cavity, large rebound phenomena are observed, usually forming a rather large cloud cavitation which moves downstream and further collapses almost in correspondence to the trailing edge. The motion of this cloud is characterised by significant spin around a direction almost parallel to the trailing edge, apparently caused by the collapse itself.

Finally it has to be mentioned that potentially erosive phenomena are observed on the whole suction side of the blades of P3, consisting in thick streak cavitation, travelling bubbles and sheet cavitation forming cloud cavitation at trailing edge. As already mentioned for propeller P2, the focus of current work is on suction side root cavitation, therefore other phenomena like blade sheet cavitation or pressure side cavitation, although generally important, are not here discussed. However it is useful to keep in mind the presence of these phenomena when analysing paint removal on the blades.

4 CAVITATION EROSION RESULTS

Results of paint tests are reported in this section with the help of photographs captured by CAM1 during tests. The damages observed in the painting of these blades gives a coherent indication of the presence of potentially erosive phenomena for all three studied test cases.

In this work, simple data such as the extent of the paint damages and the inception time of damages is analysed trying to correlate this quantity with the flow aggressiveness. The inception time of the damage is defined as the time passing from the beginning of the test to the occurrence of the first damage on the coating.

Figure 8(a) shows the suction side of blade root for propeller P1 for one of the blades, highlighting paint removal in these zones. Suction Side root/hub erosion can be seen in the red circles in the images. A consistent damage was observed for all blades, located between the fillet at the root and the surface of the hub, near the trailing edge of the root itself.

The root blade damages on suction side for propeller P2 is shown in Figure 8(b). Suction side damage on the blade root is exhibited in red circle. The damage was near the trailing edge of the blade above the overhang, and on surface of hub below the overhang, and it seems to be consistent for all four blades.

Suction side damages for P3 propeller on the blade root are shown in Figure 8(c). The suction side damage (shown in red circle) started near the mid chord of the blade root extended to the trailing edge root, and forming a streak like structure. The damage at the trailing edge blade root was a bit extended.

The damage extent on suction side for all propellers with magnified view is reported in Figure 9. For P1, the damage on suction side located on the hub/fillet was around 0.5 cm in length.

Propeller P2 damage on suction side near the trailing edge above the overhang was in the form of a quarter ellipse with major to minor axis ratio of 1 cm to 0.4 cm. The damage on the surface of hub below the overhang was a semi-circular damage of diameter of around 0.8 cm.

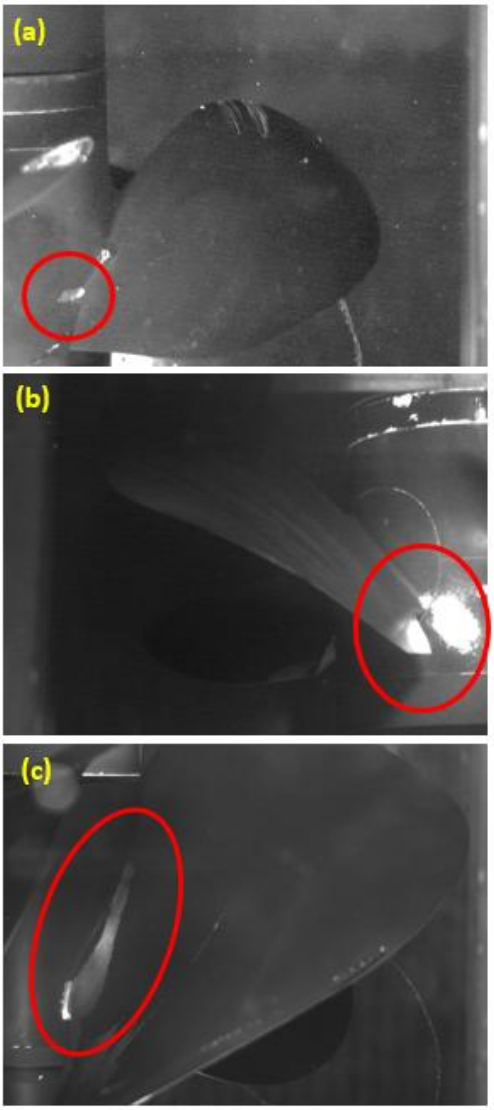

Figure 8. Damages on suction observed from CAM1 for (a) P1 Propeller (b) P2 Propeller and (c) P3 Propeller

Propeller P3 damage on suction side in the streak form has a length of around 5 cm along the root chord. The maximum damage appeared near trailing edge, with a radial extension of about 0.7 cm.

While moving to the analysis of inception time and damage extent, it must be noted that for most of the tests significant discrepancies have been observed among the blades of the same propeller. These discrepancies may be related to various causes, such as the presence of anomalous cavitation on some blades because of surface defects, or differences in the paint application. Keeping this in mind, average values are here considered to capture general trends and compare them with observed cavitation dynamics.

Table 2. Concluding parameters of present study

Propeller	Cavitation Extent	Inception Time (Minutes)	Damage Extent	
			Blade Root T.E (mm)	Hub / Fillet (mm)
P1	Low	150	-	5
P2	Medium	70	Ellipse 10 to 4	8
P3	High	15	50	-

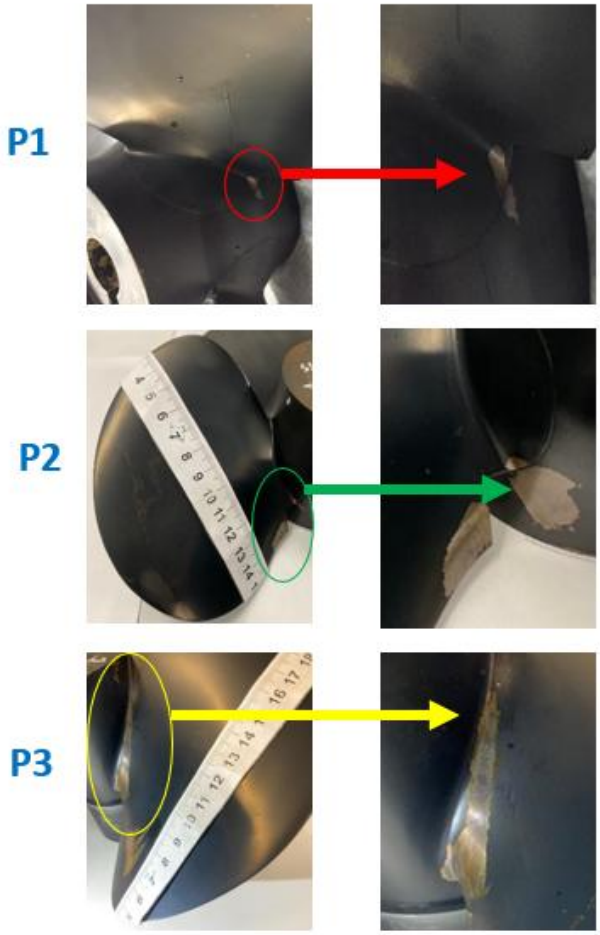

Figure 9. Damages on suction side observed after test for P1, P2 and P3 Propeller with magnified view

The average inception time of suction side root damages for propeller P1, P2 and P3 was 150, 70 and 15 minutes respectively. It can be seen that with increasing extent of cavitation, the inception time has been reduced tremendously. Analogously, the damage area, i.e. the area where paint has been removed, increases significantly from P1 to P3.

The damage inception time and the final extent of the damages depends on the main characteristics of cavitation and collapse phenomena, such as the intensity of collapse events, the number of collapse events and the area of occurrence of collapse events.

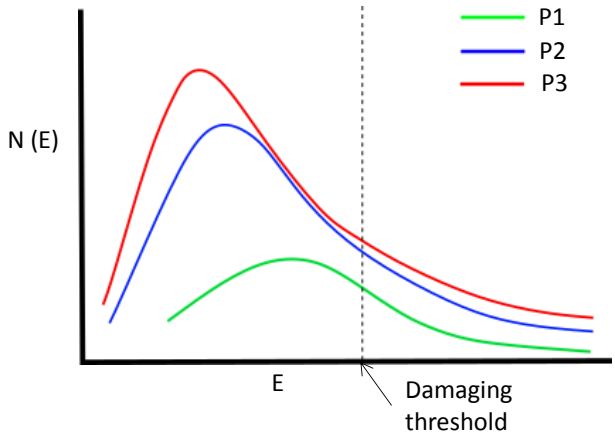

Figure 10: Schematic representation of Energy Spectra

The first two characteristics are related to the erosive power introduced by Avellan (1991). A qualitative representation of the energy spectra associated to cavity collapses, as proposed by Hammitt (1963), is shown in Figure 10. These curves are based on the interpretation of the high speed videos, without any direct measurements so they are used only to schematically support the discussion.

Basically, in all the three cases collapse events exist characterised by sufficient energy for damaging the paint layer. From this point of view, it must be underlined that the damaging threshold of the coating is not known but reasonably rather low. As a consequence, occurrence of damages on the paint does not implies overcoming the damaging threshold on the real propeller.

Having said this, P1 generates a small number of bubbles (about 1 per blade passage, on average). These cavities however are expected to be characterised by lower potential energy than those of propellers P2 and P3, but still sufficient to cause paint removal, i.e. above the paint damaging threshold. As a result, the erosive power associated to this cavitation regime is rather low and a large number of cavitation events are needed before generating visible damages on the coating.

Moving to propeller P2 and P3, the number of collapse events increase remarkably. Identifying separate collapse events into the evolution of the observed cavities is almost impossible, however the continuous destruction of cavitating sub-structures at the trailing edge of the main cavity could be assimilated to the collapse of about ten separate bubbles per blade passage for P2, even more for P3. The energy spectrum associated to these events is likely centred on lower values of the energy, but the associated power is definitely larger, resulting in faster occurrence of paint removal.

This theoretical interpretation of results does not yet take into account the effect of the collapse of the main cavity observed for P3 for each blade passage. This phenomenon, although occurring once per blade passage, it is likely characterized by very high energy, which could result in a second high energy peak in the P3 energy distribution. The phenomenon causes also secondary events of cloud cavitation occurring during the rapid contraction of the main cavity. This global collapse causes the onset of paint removal after few minutes from the beginning of tests.

The reported discussion seems to confirm the capability of energetic approaches to describe the cavitating flow aggressiveness, however data on cavitating volume is needed to rigorously apply such approaches, as proposed by Pereira (1998). The application of such approaches to present test cases, exploiting computer vision techniques as those proposed Savio (2009) will be considered for the prosecution of current research.

5 CONCLUSIONS

In this work, model scale investigations of cavitation erosion on three propeller models have been presented. The experimental procedure based on the use of soft paints combined with high speed video recordings demonstrated to be a valuable approach to detect potentially erosive phenomena. The cavitation observations have been also exploited to study the different hydrodynamic mechanisms responsible of erosion for propeller blade root cavitation. This allowed identifying different erosive phenomena:

1) Collapse of single macroscopic bubbles close to the body surface, in the form of hemispherical collapse and twisting cavities collapse.
2) Continuous collapse of macroscopic substructures and cloud cavitation at the trailing edge of larger cavitating structures.
3) Global collapse of the main cavity with its collateral phenomena such as rebounds and generation of cloud cavitation and vortexes.

The paint removal inception time and extent obtained from these tests have been used in order to investigate the opportunity to approximately measure the aggressiveness of cavitating flows by means of these simple descriptors. The scope is to sort test cases in terms of their aggressiveness in order to build empirical correlations with full scale data on propeller erosion occurrence.

Both descriptors allowed to correctly sort the considered cases, however the information carried by them is highly approximate and uncertainties associated to the paint application can jeopardize results reliability, especially in case limited differences are present, contrarily to what observed for the present three propellers.

In order to cope with these limitations, more quantitative information on cavitation volume and collapse events are needed. Accordingly, future work on this subject will take advantage of the gained understanding of erosion mechanisms for current test cases in order to suitably apply optical techniques to the characterisation of marine propeller blade root cavitation.

REFERENCES

Abbasi, A.A., Viviani, M., Bertetta, D., Delucchi, M., Ricotti, R., & Tani, G. (2022). Experimental Analysis of Cavitation Erosion on Blade Root of Controlable Pitch Propeller. In 20th International Conference on Ship & Maritime Research. Genoa - La Spazia, Italy.

Avellan, F., Dupont, P., & Farhat, M. (1991). Cavitation erosion power. In Proceedings of the Cavitation'91 Symposium, 1st ASME-JSME Fluid Engineering Conference (Vol. 116, No. CONF, pp. 135-140). The American Society of Mechanical Engineers.

Bensow, R., Bark, G., & Lu, N. X. (2012). Hydrodynamic mechanisms in cavitation erosion. In 8th International Symposium on Cavitation.

Cao, Y., Peng, X., Yan, K., Xu, L., & Shu, L. (2017, June). A qualitative study on the relationship between cavitation structure and erosion region around a 3d twisted hydrofoil by painting method. In Fifth International Symposium on Marine Propulsors. Finland.

Dular, M., & Petkovsek, M. (2015). On the mechanisms of cavitation erosion–Coupling high speed videos to damage patterns. Experimental Thermal and Fluid Science, 68, 359-370.

Franc, J. P., & Michel, J. M. (2006). Fundamentals of cavitation (Vol. 76). Springer science & Business media.

Fujikawa, S., & Akamatsu, T. (1980). Effects of the non-equilibrium condensation of vapour on the pressure wave produced by the collapse of a bubble in a liquid. Journal of Fluid Mechanics, 97(3), 481-512.

Hammitt, F. G. (1963). Observations on cavitation damage in a flowing system. NASA

ITTC (2011). Recommended Procedures and Guidelines - Cavitation Induced Erosion on Propellers, Rudders and Appendages Model Scale Experiments, p. 1-14.

Johnsen, E., & Colonius, T. I. M. (2009). Numerical simulations of non-spherical bubble collapse. Journal of Fluid Mechanics, 629, 231-262.

Koukouvinis, P., Mitroglou, N., Gavaises, M., Lorenzi, M., & Santini, M. (2017). Quantitative predictions of cavitation presence and erosion-prone locations in a high-pressure cavitation test rig. Journal of Fluid Mechanics, 819, 21-57.

Pereira, F., Avellan, F., & Dupont, P. (1998). Prediction of cavitation erosion: an energy approach. Journal of Fluid Engineering, 719-27.

Petkovsek, M., & Dular, M. (2013). Simultaneous observation of cavitation structures and cavitation erosion. Wear, 300(1-2), 55-64.

Pfitsch, W., Gowing, S., Fry, D., Donnelly, M., & Jessup, S. (2009). Development of measurement techniques for studying propeller erosion damage in severe wake field. Proceedings of the 7th International Symposium on Cavitation. Michigan, USA.

Savio, L., Viviani, M., Conti, F., & Ferrando, M. (2009). Application of computer vision techniques to measure cavitation bubble volume and cavitating tip vortex diameter. Proceedings of the 7th International Symposium on Cavitation, August 17-22, 2009, Ann Arbor, Michigan, USA.

Sreedhar, B. K., Albert, S. A., & Pandit, A. B. (2017). Cavitation damage: Theory and measurements–A review. Wear, 372, 177-196.

Tani, G., Aktas, B., Viviani, M., & Atlar, M. (2017). Two medium size cavitation tunnel hydro-acoustic benchmark experiment comparisons as part of a round robin test campaign. Ocean Engineering, 138, 179-207.

Van Rijsbergen, M., Foeth, E. J., Fitzsimmons, P., & Boorsma, A. (2012, August). High-speed video observations and acoustic-impact measurements on a NACA 0015 foil. In Proceedings of the 8th International Symposium on Cavitation, Singapore (pp. 13-16).